Financial support provided by the Swedish Natural Science Research Council and the Lennander foundation is gratefully acknowledged.

References

AGRON, P. A., BUSING, W. R. & LEVY, H. A. (1972). Abstracts. Winter Meet. Am. Crystallogr. Assoc., Albuquerque, New Mexico, p.52.

ALCOCK, N. W. (1971). *Acta Cryst.* B**27**, 1682–1683.

BECKER, P. & COPPENS, P. (1974). *Acta Cryst.* A**30**, 129–147.

BECKER, P. & COPPENS, P. (1975). *Acta Cryst.* A**31**, 417–425.

BUSING, W. R. (1975). Private communication.

COPPENS, P. & HAMILTON, W. C. (1970). *Acta Cryst.* A**26**, 71–83.

CRAVEN, B. M. & MCMULLAN, R. K. (1979) *Acta Cryst.* B**35**, 934–945.

HERMANSSON, K. & LUNELL, S. (1981). *Chem. Phys. Lett.* **80**, 64–68.

HERMANSSON, K. & LUNELL, S. (1982). *Acta Cryst.* B**38**, 2563–2569.

HERMANSSON, K. & THOMAS, J. O. (1979). Abstracts. Fifth Eur. Crystallogr. Meet., Copenhagen, Denmark, p. 351.

HERMANSSON, K., THOMAS, J. O. & OLOVSSON, I. (1980). *Acta Cryst.* B**36**, 1032–1040.

HIRSHFELD, F. L. (1971). *Acta Cryst.* B**27**, 769–781.

HIRSHFELD, F. L. (1977). *Isr. J. Chem.* **16**, 168–174.

International Tables for X-ray Crystallography (1974). Vol. IV, pp. 72–73, 149. Birmingham: Kynoch Press.

KOESTER, L. & STEYERL, A. (1977). *Neutron Physics*, p. 36. Berlin, Heidelberg, New York: Springer.

LEHMANN, M. S. & LARSEN, F. K. (1974). *Acta Cryst.* A**30**, 580–584.

LUNDGREN, J.-O. (1979*a*). *Crystallographic Computer Programs*. Report UUIC-B13-04-04, Institute of Chemistry, Univ. of Uppsala.

LUNDGREN, J.-O. (1979*b*). *Acta Cryst.* B**35**, 1027–1033.

MAIR, S. L. (1978). *Acta Cryst.* A**34**, 542–547.

PEPINSKY, R. (1939). *Z. Kristallogr.* **102**, 119–131.

RABAUD, H. & GAY, R. (1957). *Bull. Soc. Fr. Minéral. Cristallogr.* **80**, 166–180.

REES, B. (1977). *Isr. J. Chem.* **16**, 180–186.

STEVENS, E. D. & COPPENS, P. (1980). *Acta Cryst.* B**36**, 1864–1876.

THORNLEY, F. R. & NELMES, R. J. (1974). *Acta Cryst.* A**30**, 748–757.

ZACHARIASEN, W. H. (1967). *Acta Cryst.* **23**, 558–564.

Acta Cryst. (1982). B**38**, 2563–2569

The Theoretical Electron Density in Lithium Hydroxide Monohydrate*

BY KERSTI HERMANSSON

Institute of Chemistry, University of Uppsala, Box 531, *S*-751 21 *Uppsala, Sweden*

AND STEN LUNELL

Department of Quantum Chemistry, University of Uppsala, Box 518, *S*-751 20 *Uppsala, Sweden*

(*Received* 28 *August* 1981; *accepted* 3 *March* 1982)

Abstract

The electron density in $LiOH.H_2O$ has been determined by *ab initio* MO–LCAO–SCF calculations. All nearest neighbours to the H_2O molecule and the OH^- ion, respectively, have been included explicitly in the calculations; next-nearest and more-distant neighbours have been simulated by point charges. The theoretical electron density maps are compared with experimental maps [Hermansson & Thomas (1982). *Acta Cryst.* B**38**, 2555–2563] with good overall agreement. The influence of intermolecular bonding in the crystal is found to be twofold. Firstly, the overall polarization of the H_2O molecule and the OH^- ion is increased significantly. Secondly, the electron density around the O nuclei in H_2O and OH^- is rearranged, leading to a decrease of density in the lone-pair directions. The reasons for this decrease are discussed in some detail.

Introduction

This paper is part II of an experimental and theoretical study of the electron density in $LiOH.H_2O$.

In part I (Hermansson & Thomas, 1982), the redistribution of electrons occurring on bond formation in $LiOH.H_2O$ was discussed in terms of deformation density maps. These displayed the deviation of the total experimental electron density from a calculated reference state of superposed spherically averaged

* Hydrogen Bond Studies. CXLV.

0567-7408/82/102563-07$01.00

atoms or ions. In the present paper, the experimental maps are compared with corresponding theoretical maps obtained from quantum-mechanical *ab initio* MO–LCAO–SCF calculations.

We have also calculated deformation maps where the reference state subtracted from the total theoretical density consists of a superposition of $\rho(H_2O)$, $\rho(OH^-)$ and $\rho(Li^+)$, instead of the free spherically averaged atoms. Such maps display the influence of the surroundings on the molecular electron densities more clearly than the conventional deformation density maps. A preliminary discussion of the interpretation of such maps for the H_2O molecule in LiOH.H_2O can be found in an earlier paper (Hermansson & Lunell, 1981).

One reason for the choice of LiOH.H_2O for a comparative experimental and theoretical electron density study is that its crystal structure renders it amenable to *ab initio* calculations in which the nearest neighbours of both the H_2O molecule and OH^- ion can be included explicitly in the calculations. This facilitates a more rigorous study of the effects of intermolecular bonding on molecular constituents than would be the case if the crystal environment were simulated, for example, by point charges.

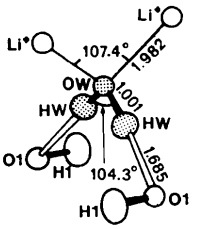

Fig. 1. The environment of the H_2O molecule in LiOH.H_2O. The O(W) atom lies on a twofold rotation axis. Distances (Å) and angles are taken from neutron diffraction data.

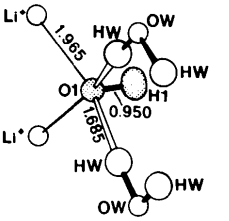

Fig. 2. The environment of the OH^- ion in LiOH.H_2O. The OH^- ion lies in a mirror plane. Distances (Å) are taken from neutron diffraction data.

Computational method

Ab initio MO–LCAO–SCF calculations were carried out both for the H_2O molecule and for the OH^- ion, each together with their immediate surroundings as they occur in the LiOH.H_2O crystal. The two complexes calculated were thus $(Li^+)_2(OH^-)_2.H_2O$ ('water complex', see Fig. 1) and $(Li^+)_2(H_2O)_2.OH^-$ ('hydroxide complex', see Fig. 2); each contains 34 electrons. All neighbours to the water complex out to a distance of 5·8 Å from the water O atom were included in the calculations as point charges at the atomic sites (88 charges in all). The charges were taken from a Mulliken population analysis of the $(Li^+)_2(OH^-)_2.H_2O$ wavefunctions and were modified in an iterative way until the Mulliken charges derived from the final wavefunctions were identical to the point charges used in reproducing the crystal environment. For the hydroxide complex, 87 atoms (out to a distance of 5·8 Å from the hydroxide O atom) were included as point charges which were derived by a similar iterative procedure.

The geometries were kept fixed throughout the calculations; the atomic coordinates were taken from the neutron diffraction data refinement (Neutron 1, see part I). A stereoscopic picture of the unit cell is shown in Fig. 2 of part I and a list of distances and angles is given in Table 4 of the same paper.

The quantum-mechanical calculations were made with the program system *MOLECULE* (Almlöf, 1972). The basis sets consisted of contracted Gaussian-type functions of DZP quality or better. For the *water complex*, the (10*s*6*p*/5*s*) basis set of Dunning (1971) contracted to ⟨5*s*3*p*/3*s*⟩ was used for the O(W) and H(W) atoms (with a scale of factor of 1·49 for the H exponent), augmented with polarization functions according to Roos & Siegbahn (1970). Somewhat smaller basis sets were chosen for the hydroxide ion in the water complex; namely Dunning's (1970) (9*s*5*p*/4*s*) basis set contracted to ⟨4*s*2*p*/2*s*⟩ with a scale factor of 1·12 for the H exponent, and one polarization function on H [as for H(W)] but no polarization function on the O atom. The extended basis described above was also used for the O(1) and H(1) atoms of the *hydroxide complex*, whereas the smaller basis was applied to the O(W) and H(W) atoms. The basis set used for Li^+ in all calculations was the (10*s*) set of Dunning (1971) contracted to ⟨5*s*⟩ and augmented with a 2*p* function with exponent 0·525. The latter value was obtained by minimization of the energy of a free $Li^+.H_2O$ complex. The energy obtained for a free water molecule in its equilibrium geometry (0·957 Å, 104·5°) using the extended basis was −76·05591 a.u. (1 a.u. ≡ 4·3564 × 10^{-18}J).

For checking purposes, calculations were also carried out in which the total basis sets for the entire complexes were used for the individual OH^- and H_2O fragments to be subtracted in the difference maps. This avoids any spurious effects arising from an improved description of a particular fragment due to the presence of extra basis functions on neighbouring fragments. This correction was, however, found to be irrelevant to the appearance of the density maps.

The final Mulliken charges obtained for the water complex in the iterative procedure described above

were: Li +1·00, O(1) −1·24, O(W) −0·87, H(1) +0·28 and H(W) +0·42. The final Mulliken charges were Li +0·99, O(1) −1·27, O(W) −0·75, H(1) +0·43 and H(W) +0·34 for the hydroxide complex. It can be noted that the charges obtained in the two calculations differ somewhat. One reason is that the environment of a particular molecular unit was represented in different ways in the two calculations (partly by explicit inclusion and partly by point charges). Another reason is that each molecular entity was described with a basis set which was larger when it occurred as a central molecule than when it occurred as a ligand. Part of the discrepancy therefore has its roots in the well known basis-set dependence of the Mulliken population analysis, since the differences in the actual electron densities for, say, a water molecule calculated in the two different ways are, in fact, rather small. [This can be seen by comparison of Figs. 4(*a*) and 4(*b*); both show the deformation density in the hydrogen-bond region. Fig. 4(*a*) is obtained from the calculation on the water complex, while Fig. 4(*b*) is derived from the hydroxide-complex calculation.] Since the point charges all describe next-nearest and still-more-distant neighbours, however, the charge distribution of the central molecule (ion) is quite insensitive to their detailed values. Thus, no changes were found in the deformation density maps when the point charges used for O(1) and H(1) in the water-complex calculation were taken from the hydroxide-complex calculation (*i.e.* −1·27 and +0·43, respectively) instead of the values used in the iterative procedure described above (*i.e.* −1·24 and +0·28).

Results and discussion

Deformation maps – reference states

Most deformation maps published display the total (experimental or theoretical) electron density minus the superposition of free spherical (or spherically averaged) atoms. Such maps show the total deviation of the electron density in the crystal from a sum-of-free-atoms state, *i.e.* they display the combined effect of intra- and intermolecular bonding, where the former is usually the far more dominant effect. This complicates the interpretation of the maps when interest is focused on the weaker effects of intermolecular bonding. A more suitable reference state for such analyses is the superposition of the electron densities of the relevant molecular constituents (with the experimental geometry of the crystal).

Since the molecules/molecular ions entering a crystal in general do not have identically the same geometry as in the free state, the influence of the crystalline environment on the electron density of a particular molecular unit will be both indirect, caused by the changes in internal geometry, and direct. Formally, one can consider the crystal formation to proceed in two steps. In the first step, the geometry of the molecules/ions is changed from that of the free state to that in the crystal. In the second step, these units are assembled to form the crystal. Each of the steps is accompanied by a redistribution of the electron density.

In principle, the decomposition of the crystal formation into two non-physical processes suffers from the drawback that the intermediate step consists of molecules/ions where the atoms are in non-equilibrium positions. This, in turn, may introduce artificial features in the electron density. In the present case, however, the density changes accompanying the first step are almost one order of magnitude smaller than those in the second step. For all practical purposes it is therefore sufficient to consider only the latter, when discussing the intermolecular interactions in the $LiOH.H_2O$ crystal. This is the approach taken in the present paper. However, it cannot be excluded that the density changes occurring in the first step can be more important in other systems.

Static versus dynamic maps

The experimental diffraction studies of $LiOH.H_2O$ were carried out at 295 K. A comparison of experimental and theoretical electron densities requires *either* that the effects of nuclear thermal motion are removed from the experimental dynamic density, for example by a deconvolution process (see, *e.g.*, Stewart, 1969; Hirshfeld, 1971), *or* that the theoretical static density is smeared by thermal motion (Hase, Reitz & Schweig, 1976; Coppens & Stevens, 1977). The merits and disadvantages of the two approaches have been discussed by several authors, *e.g.* Coppens & Stevens (1977). In the present case the method of Hirshfeld (1971) was used to obtain the experimental static deformation maps.

Comparison of experimental and theoretical deformation maps

In part I the experimental deformation density for $LiOH.H_2O$ was displayed in several sections through the H_2O molecule [Fig. 3(*a*)–(*c*) of part I], through the O(W)–H(W)···O(1) hydrogen bond [Fig. 4(*a*)–(*c*)] and through the OH^- ion [Fig. 5(*a*)–(*c*)]. These maps show the total electron density minus the superposition of free spherical (or spherically averaged) atoms or ions (O, H and Li^+). Figs. 3–5 of the present paper show the corresponding theoretical maps [*i.e.* figures to be compared have the same numbering in both papers; note, however, that Fig. 4(*a*) (part I) corresponds to both Figs. 4(*a*) and 4(*b*) (this paper), while Figs. 4(*b*) and 4(*c*) (part I) do not have counterparts in this paper].

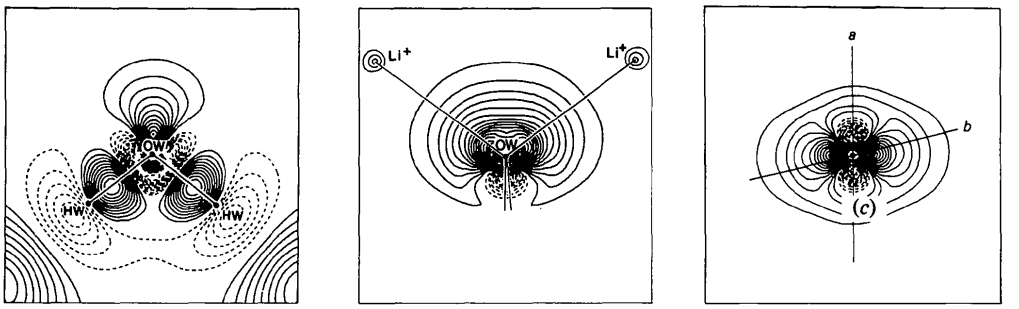

(a) (b) (c)

Fig. 3. Static theoretical deformation density for the $(Li^+)_2(OH^-)_2.H_2O$ complex. The contour interval is 0·05 e Å^{-3}. Negative contours are dashed and the zero contour is omitted. The same contour levels will be used in all figures. The substracted reference atoms or ions in Figs. 3–7 are Li^+, O and H. (*a*) Section through the H_2O molecular plane. (*b*) Section through the Li^+–O(*W*)–Li^+ plane. (*c*) Section through a plane normal to the bisector of the H(*W*)–O(*W*)–H(*W*) angle and passing through the O(*W*) atom. The line *a* indicates the positions of the projections of the H(*W*) atoms onto the plane. The line *b* indicates the positions of the projections of the Li^+ ions onto the plane. Note that the experimental map corresponding to this figure (*i.e.* Fig. 3*c* of part I) is taken in a plane passing 0·25 Å above the O(*W*) atom. These sections were chosen since the lone-pair maxima are situated much further out from the O(*W*) atom in the experimental map.

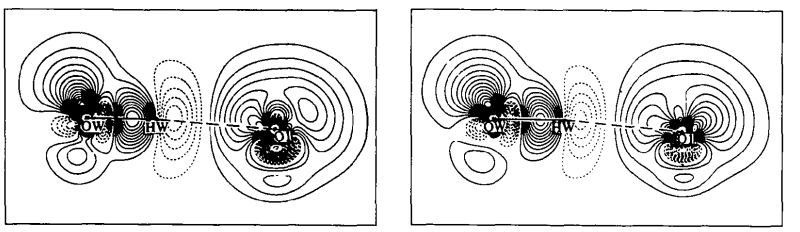

(a) (b)

Fig. 4. Static theoretical deformation density through the hydrogen bond [O(*W*)–H(*W*)···O(1)]. (*a*) Deformation density derived from the calculation on the $(Li^+)_2(OH^-)_2.H_2O$ complex. (*b*) Deformation density derived from the calculation on the $(Li^+)_2(H_2O)_2.OH^-$ complex.

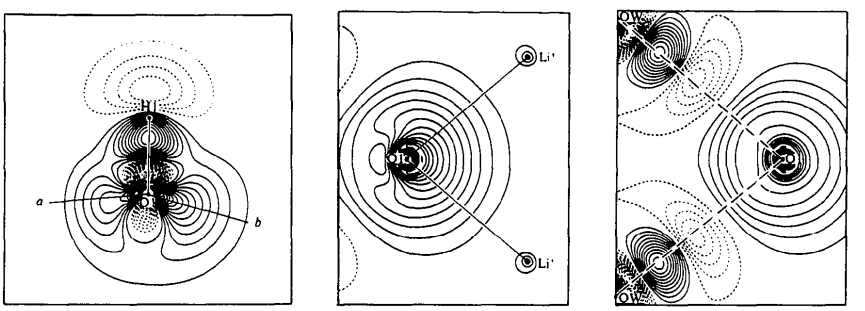

(a) (b) (c)

Fig. 5. Static theoretical deformation density for the $(Li^+)_2(H_2O)_2.OH^-$ complex. (*a*) In the mirror plane containing OH [line *a* indicates the intersection with a plane containing the two O(*W*) neighbours and line *b* the intersection with a plane containing the two Li^+ neighbours]. (*b*) In the Li^+–O(1)–Li^+ plane. (*c*) In the O(*W*)···O(1)···O(*W*) plane.

The agreement between experimental and theoretical maps for $LiOH.H_2O$ is generally good. This is true in particular of the bonding regions within the H_2O molecule and the OH^- ion, and of the hydrogen-bond region (see also Table 1). The experimental and theoretical deformation maps differ more in the lone-pair regions of the O atoms; there is markedly less density in the experimental maps close to the O nuclei, even though at a distance greater than 0·5 Å from the O nuclei the agreement is much better [see the planes through Li^+–O(*W*)–Li^+, Li^+–O(1)–Li^+ and O(*W*)···O(1)···O(*W*)]. As was discussed in part I, a major part of this discrepancy is probably caused by errors in the experimental maps.

When considering Table 1, it should be kept in mind that the experimental deformation density within, say,

Table 1. *Comparison of experimental and theoretical peak heights in the deformation maps* (e Å^{-3})

	Experiment		Theory
	Dynamic	Static	Static
O(*W*)–H(*W*)	0·31	0·66	0·55
O(1)–H(1) bond	0·22	0·49	0·58
O(*W*) lone pair [Li$^+$–O(*W*)–Li$^+$ plane]	0·17	(0·22)	0·97
O(1) lone pair [O(*W*)–O(1)–O(*W*) plane]	0·19	(0·27)	0·60
O(1) lone pair [Li$^+$–O(1)–Li$^+$ plane]	0·21	(0·27)	0·63
H(*W*)···O(1) bond	−0·14	−0·24	−0·29
H(1)···O(1) bond	−0·17	−0·22	−0·25

0·3 Å of the nuclei is extremely unreliable. As Figs. 3–5 show, however, the O lone pairs have their maxima just in this region. A comparison of experimental and theoretical *peak heights* is therefore meaningless for the lone pairs, and one has to be satisfied with a comparison of the general shape of the deformation densities at larger distances from the O nuclei. The static experimental peak heights for the lone pairs have therefore been put within parentheses in Table 1, in order to emphasize that the actual position of the peak is an artifact caused by the impossibility of performing reliable measurements close enough to the nucleus.

Influence of intermolecular bonding

Deformation density maps where spherical-atom densities are subtracted from the total density are strongly dominated by intramolecular bonding effects. This is clearly seen if the deformation densities in Figs. 3(*a*)–(*c*) and 5(*a*) are compared with the corresponding deformation densities for the free H_2O molecule and OH^- ion, respectively, in Figs. 6(*a*)–(*c*) and 7 (see also Hermansson & Lunell, 1981). As a consequence of this, the maxima in the O lone-pair deformation densities are not situated along the O–ligand directions. This is particularly well demonstrated for the water molecule (Fig. 3*c*).

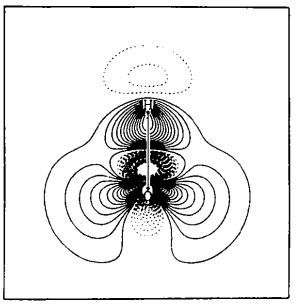

Fig. 7. Static theoretical deformation density for a free OH^- ion with the same geometry as in $LiOH.H_2O$.

The explicit influence of the crystal surroundings on the electron densities of H_2O and OH^- is displayed in Figs. 8(*a*)–(*c*) and 9(*a*)–(*c*), where the isolated H_2O, OH^- and Li^+ constituents (in the geometry of the crystal) are subtracted from the total (theoretical) density. The dominant effect of the surroundings on H_2O and OH^- is a shift of electron density away from the H atoms towards the O atom. For the H_2O molecule, this can best be seen in Fig. 8(*a*), and is not unexpected, in view of the geometrical arrangement of the surrounding positive and negative ions (*cf.* Fig. 1).

The changes in the electron density are of about the same magnitude in the OH^- ion as in the H_2O molecule [in fact, somewhat larger in the former; *cf.* Figs. 8(*a*) and 9(*a*)], even though the polarizing field may be expected to be somewhat weaker at the OH^- ion (*cf.* Figs. 1 and 2). The obvious reason for this is that, like all negative ions, the OH^- ion is rather easy to polarize because of its loosely bound extra electron.

In addition to this overall polarization of the H_2O molecule and OH^- ion, significant local rearrangements of electron charge can be observed around the O nuclei. This is seen particularly well in Fig. 8(*b*), which shows the influence of the environment in the Li^+–O(*W*)–Li^+ plane (approximately the lone-pair plane of the water molecule) and in Fig. 9(*a*)–(*c*),

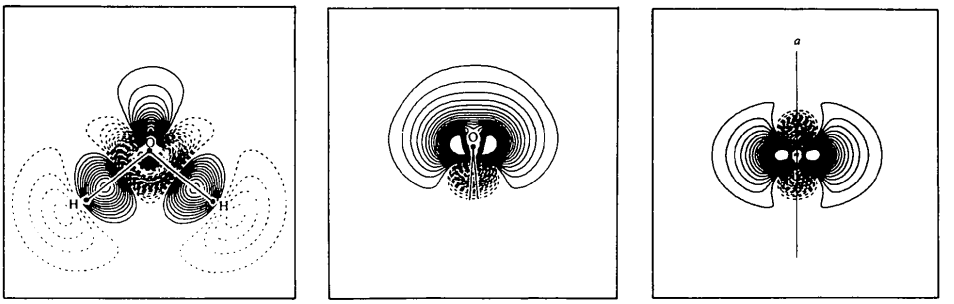

(*a*) (*b*) (*c*)

Fig. 6. Static theoretical deformation density for a free H_2O molecule with the same geometry as in $LiOH.H_2O$. (*a*) In the molecular plane. (*b*) Section through the O atom and perpendicular to the molecular plane. (*c*) Section through a plane normal to the bisector of the H–O–H angle and passing through the O atom. The line *a* indicates the projection of the H atoms onto the plane.

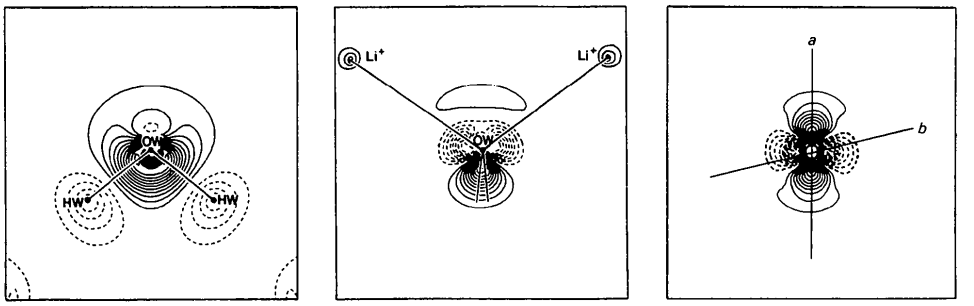

(*a*) (*b*) (*c*)

Fig. 8. $\rho_{tot} - (\rho_{H_2O} + 2\rho_{OH^-} + 2\rho_{Li^+})$ static theoretical deformation density for the $(Li^+)_2(OH^-)_2.H_2O$ complex (same sections as in Fig. 3).

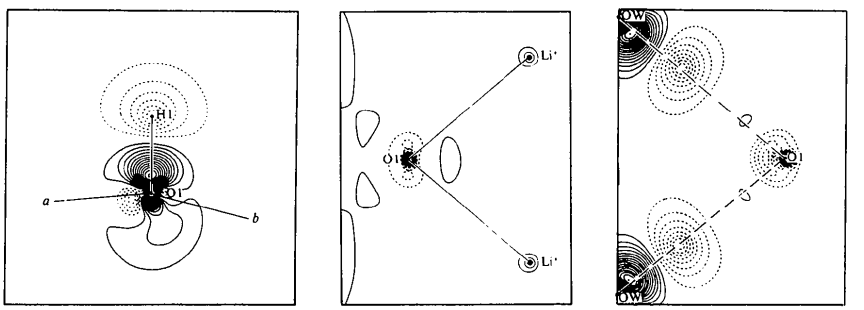

(*a*) (*b*) (*c*)

Fig. 9. $\rho_{tot} - (\rho_{OH^-} + 2\rho_{H_2O} + 2\rho_{Li^+})$ static theoretical deformation density for the $(Li^+)_2(H_2O)_2.OH^-$ complex (same sections as in Fig. 5).

which show the influence of the environment on the OH^- ion. An interesting observation that can be made from Figs. 8(*b*) and 9(*a*)–(*c*) is that the lone-pair electron density in the directions of incoming bonds is, in fact, significantly decreased by the influence of the surroundings. This is true both for the H_2O molecule and OH^- ion in $LiOH.H_2O$, and has been observed also in some other cases (see Hermansson & Lunell, 1981, for references).

There are at least two mechanisms which can contribute to this decrease in lone-pair density. On the one hand, there is a direct attraction between the O lone-pair electrons and the Li^+ ions [or hydrogen-bonding H(*W*) atoms]. This causes an outward shift of electron density which can be observed in Figs. 8(*b*), 9(*b*) and 9(*c*) as extended regions of low electron excess ($<0{\cdot}10$ e Å^{-3}) in the regions between the O atoms and the Li^+ ions or H(*W*) atoms. On the other hand, the lone-pair features of the *free* H_2O molecule and OH^- ion arise only as a consequence of O–H bond formation, *i.e.* as a response to the non-spherical environment of the O atoms. In the crystal, the surroundings of the O atoms are much more nearly spherically symmetric than in the free molecule (ion), with the result that the electron redistribution within H_2O and OH^- occurring upon covalent-bond formation (Figs. 6 and 7) will be partially reversed in the crystal. This is indeed seen to be the case; regions of electron excess in Figs. 6 and 7 correspond roughly to regions of electron deficiency in Figs. 8 and 9(*a*), and *vice versa*. The existence of this indirect effect on the lone-pair density is also shown by the fact that an electron redistribution very similar to that shown in Fig. 9(*a*)–(*c*) is obtained if the surrounding ions are omitted in the calculations and, instead, the H nuclear charges are reduced to cause a shift in the O–H bond electrons towards the O atom.

One can observe that the directions of maximum decrease of the O(*W*) lone pairs (*cf.* Fig. 8*c*) do not lie in the Li^+–O(*W*)–Li^+ plane, but rather in a plane perpendicular to the H(*W*)–O(*W*)–H(*W*) bonds (the angle between these planes is 12°). The total electron density of a water molecule is itself very nearly spherical in the whole lone-pair region (see, *e.g.*, Olovsson, 1980, Fig. 6). There is therefore no particular reason why the decrease in electron density close to the O nucleus, which would accompany a purely electrostatic attraction towards the Li^+ ions or hydrogen-bonding H(*W*) atoms, should be noticeably larger in the directions of the lone-pair maxima (perpendicular to the molecular plane) than in other directions in the lone-pair region. The electron redistribution observed

thus stresses the significance of an electron flow dominated by the internal geometry of the water molecule and not by the direct influence of the Li^+ ions.

Without making a careful integration over different regions of the electron density maps, it is difficult to judge the relative importance of the two above-mentioned mechanisms, *i.e.* whether most of this lone-pair density flows out in the directions of the positive neighbours to form the extended regions of low electron excess at some distance from the O atom [Figs. 8(*b*), and 9(*b*) and (*c*)] or whether most of it is merely angularly redistributed around the O atom.

The total effect of the crystalline environment on the water molecule is a rather drastic increase of its dipole moment in the crystal compared to the free state. Because of the inherent arbitrariness in defining a strict boundary of a molecule in a crystal, its dipole moment can only be approximately calculated. By extracting the relevant parts of the wavefunction for the total $(Li^+)_2(OH^-)_2.H_2O$ complex, it can, however, be estimated that the dipole moment increases by about 60% with respect to the value for a free water molecule. This is a distinctly larger increase than is usual in other environments. The water dimer, for example, has a dipole moment which is ~20% larger than the vector sum of two H_2O molecules (Dyke & Muenter, 1974). On the other hand, the geometrical arrangement of positive and negative ions in $LiOH.H_2O$, in conjunction with the small radius of the Li^+ ions, is such that an unusually strong polarization of the water molecule is to be expected.

Finally it should be pointed out, concerning the use of the results from the present theoretical analysis for the interpretation of the experimental deformation maps of $LiOH.H_2O$, that the effects of intermolecular bonding in experimentally accessible regions are modest but not negligible. The increase in the polarization of the H_2O molecule and the OH^- ion due to the influence of the hydrogen bonds and Li^+—O contacts is clearly visible in the experimental deformation maps {compare, for example, the regions around the H(*W*) and H(1) atoms in the experimental and theoretical maps [Figs. 3(*a*) and 5(*a*) in both part I and the present paper] with the theoretical deformation densities for the free H_2O molecule and OH^- ion [Figs. 6(*a*) and 7 in this paper]}. The major effects of intermolecular bonding on the electron density in the lone-pair regions of the O atoms show up within ~0·5 Å from the O nuclei; such features may be more difficult to study experimentally.

Conclusions

The $LiOH.H_2O$ system has several properties which make it suitable for a comparative experimental and theoretical study. Firstly, it has a high valence/core electron ratio which facilitates accurate experimental electron density work. Secondly, it contains only light atoms which allows reasonably accurate theoretical calculations. Thirdly, and perhaps most importantly, the intermolecular interactions (hydrogen-bond and ion-dipole) are potentially strong enough for their effects to be observable in the deformation density maps.

We have found that, on the whole, the agreement between the experimental and theoretical densities is satisfactory. In both cases, the dominant features in the deformation density maps are due to the electron redistribution occurring on formation of the covalent bonds *within* the H_2O molecule and OH^- ion.

A further analysis of the theoretical electron density, which extracts the effects of intermolecular interactions, shows that both the water molecule and the hydroxide ion are polarized by the surroundings, so that negative charge in both cases is shifted from the H to the O atoms. In addition, the lone-pair densities associated with the O atoms are decreased in the directions of the incoming hydrogen bonds and Li—O contacts. Different mechanisms may be involved in this charge redistribution. Calculations on model systems with different geometrical surroundings should give further information about the relative importance of such mechanisms, and are being planned for the near future.

We wish to thank Professor Ivar Olovsson for his interest in this work. We are also grateful to our colleagues at the Institute of Chemistry for inspiring discussions. This work has been partly supported by grants from the Swedish Natural Science Research Council which are gratefully acknowledged.

References

ALMLÖF, J. (1972). USIP Rep. 72–09. Univ. of Stockholm, Sweden.

COPPENS, P. & STEVENS, E. D. (1977). *Isr. J. Chem.* **16**, 175–179.

DUNNING, T. H. (1970). *J. Chem. Phys.* **53**, 2823–2833.

DUNNING, T. H. (1971). *J. Chem. Phys.* **55**, 716–723.

DYKE, T. R. & MUENTER, J. S. (1974). *J. Chem. Phys.* **60**, 2929–2930.

HASE, H.-L., REITZ, H. & SCHWEIG, A. (1976). *Chem. Phys. Lett.* **39**, 157–159.

HERMANSSON, K. & LUNELL, S. (1981). *Chem. Phys. Lett.* **80**, 64–68.

HERMANSSON, K. & THOMAS, J. O. (1982). *Acta Cryst.* B**38**, 2555–2563.

HIRSHFELD, F. L. (1971). *Acta Cryst.* B**27**, 769–781.

OLOVSSON, I. (1980). *Electronic and Magnetic Distributions in Molecules and Crystals*, edited by P. BECKER. New York: Plenum.

ROOS, B. & SIEGBAHN, P. (1970). *Theor. Chim. Acta*, **17**, 199–208.

STEWART, R. F. (1969). *J. Chem. Phys.* **51**, 4569–4577.